



LAWRENCE
LIVERMORE
NATIONAL
LABORATORY

Exploration of the Versatility of Ring Opening Metathesis Polymerization: an Approach for Gaining Access to Low Density Polymeric Aerogels

S. H. Kim, M. A. Worsley, C. A. Valdez, S. J. Shin, C.
Dawedeit, T. Braun, S. O. Kucheyev, K. J. J. Wu, J.
Biener, J. H. Satcher, A. V. Hamza

November 23, 2011

RSC Advances

Disclaimer

This document was prepared as an account of work sponsored by an agency of the United States government. Neither the United States government nor Lawrence Livermore National Security, LLC, nor any of their employees makes any warranty, expressed or implied, or assumes any legal liability or responsibility for the accuracy, completeness, or usefulness of any information, apparatus, product, or process disclosed, or represents that its use would not infringe privately owned rights. Reference herein to any specific commercial product, process, or service by trade name, trademark, manufacturer, or otherwise does not necessarily constitute or imply its endorsement, recommendation, or favoring by the United States government or Lawrence Livermore National Security, LLC. The views and opinions of authors expressed herein do not necessarily state or reflect those of the United States government or Lawrence Livermore National Security, LLC, and shall not be used for advertising or product endorsement purposes.

Exploration of the Versatility of Ring Opening Metathesis Polymerization: An Approach for Gaining Access to Low Density Polymeric Aerogels

Sung Ho Kim,^{a,*} Marcus A. Worsley,^a Carlos A. Valdez,^a Swanee J. Shin,^b Christoph Dawedeit,^b Tom Braun,^b Theodore F. Baumann,^a Stephan A. Letts,^b Sergei O. Kucheyev,^b Kuang Jen J. Wu,^b Juergen Biener,^b Joe H. Satcher, Jr.,^a and Alex V. Hamza^b

^a Chemical Sciences Division, Lawrence Livermore National Laboratory, 7000 East Avenue, Livermore, CA 94550, USA

^b Nanoscale Synthesis and Characterization Laboratory, Lawrence Livermore National Laboratory, 7000 East Avenue, Livermore, CA 94550, USA

Corresponding Author

Sung Ho Kim, Ph. D.

E-mail: kim61@llnl.gov, Phone: +1-925-423-2072

P. O. Box 808, L-235, Lawrence Livermore National Laboratory, 7000 East Avenue,
Livermore, CA 94550, USA

ABSTRACT

We report the preparation of low density polymeric aerogels using the ring opening metathesis polymerization (ROMP) approach to copolymerize dicyclopentadiene (DCPD) with norbornene-based monomers (NB-R) employing a first generation Grubbs' Ruthenium-based catalyst. The ROMP approach offers an attractive synthetic method that enables the fabrication of low-density ($0.02\text{-}0.05\text{ g/cm}^3$), uniform thickness aerogel coatings on non-planar substrates. First, we explore the effect of crosslinking in the polymer backbone on the uniformity of the gel coatings formed under shear by either adding a multi-norbornene based crosslinker ($\text{NB}_n\text{-R}$) to increase, or linear NB-R co-monomers to decrease, the degree of crosslinking, respectively. We observed that adding linear monomers dramatically improved the uniformity of the gel films which we attribute to cross-linking induced changes in the rheological properties at the gel point. Second, the copolymerization of DCPD and NB-R with a different pendant group also causes a significant change in the morphology of PDCPD-based aerogels by modifying lengths of strands in the fibrous polymer network. The effect of NB-R addition on the pore structure of the aerogels is discussed in context of a molecular and interparticle crosslinking model. Finally, (bis)iodo-norbornene was synthesized to demonstrate the feasibility to fabricate functionalized aerogels by using our copolymerization approach. Our results highlight the potential of the ROMP-based copolymerization approach as a facile and versatile route to functionalized low density polymeric aerogels.

KEYWORDS. aerogels, ring opening metathesis polymerization (ROMP), dicyclopentadiene, norbornene, copolymer, crosslinking

1. Introduction

Aerogel materials with large intrinsic surface areas and ultralow densities have become attractive candidates for a wide range of applications including supercapacitors and batteries, thermal/electrical insulators, advanced catalyst supports, absorbents and carriers, and hydrogen storage.¹⁻⁴ Organic and polymeric aerogels were first reported as the counterpart of inorganic aerogels.⁵⁻⁹ The sol-gel synthesis of inorganic aerogels typically involves the transformation of molecular precursors into highly cross-linked inorganic gels that are subsequently dried using special techniques (*i.e.*, supercritical drying, freeze drying, etc.) in order to preserve their tenuous solid network. In a similar fashion, the preparation of organic and polymeric aerogels has been achieved by either (i) physical phase inversion (or coagulation) of polymers from a liquid phase to solids by changing solvent/non-solvent pairs or (ii) polymerization of multi-functional organic species into three-dimensional cross-linked polymer networks.⁵⁻⁹ While most of previous work has focused on the utilization of bulk aerogels, we are currently exploring the fabrication of low-density, uniform thickness (from 10 μm to 100 μm) aerogel coatings on the inside of cylindrical and spherical substrates.^{10,11} Such porous polymer coatings open the door to many interesting new applications such as superhydrophobic surfaces, anti-reflection coatings, column chromatography, and porous polymer membranes.¹² Our specific interest is for the fabrication of inertial confinement fusion (ICF) targets.¹¹ These targets consist of a small spherical capsule, whose inside wall is coated with a thin layer of a low density foam that is used (i) to support and define the shape of the cryogenic liquid or solid hydrogen fuel for the fusion reaction and/or (ii) as a scaffold to support dopants for diagnostics. Briefly, our strategy to fabricate aerogel coatings consists of filling a prefabricated shell with the required amount of the sol precursor followed by continuous rotation of the shell to form a smooth layer of a uniform thickness during the gel formation.¹¹ Cross-linking provides the required control over the viscosity of the precursor solution at the sol-gel transition.

Here, we use the ring opening metathesis polymerization (ROMP) approach for the synthesis of polymeric aerogels. To our knowledge, there have only been a few previous examples of applying the ROMP approach to prepare bulk porous aerogel materials.^{13,14} Lee et al. first demonstrated the feasibility of polydicyclopentadiene (PDCPD) aerogels as new insulation materials.¹³ Leventis et al. reported a novel low temperature synthetic route to extremely robust polyimide aerogels via ROMP of a crosslinkable norbornene end-capped diimide monomer.^{14a} Although these works demonstrate the ability to produce monolithic aerogels, our goal of forming uniform aerogel coatings adds another layer of complexity. For example, the coating of non-planar surfaces with thin and homogeneous aerogel films requires continuous rotation of the object to be coated. Without a proper control over viscosity and gel time, shear forces can damage the growing gel networks and prevent the formation of uniform coating.¹⁰ Using the example of polydicyclopentadiene-based gels, we demonstrate that both moduli and viscosity at a gel point can be tuned by modifying the degree of cross-linking through copolymerization of dicyclopentadiene (DCPD) with a linear norbornene co-monomer. The effect of monomer addition on the morphology of the resulting aerogels was investigated by using substituted norbornene monomers (NB-R) with various pendant groups R. Finally, (bis)iodo-norbornene monomer was added to demonstrate the fabrication of functionalized aerogels and to give further quantitative understanding on this copolymerization process. The goal of our study is to provide a simple and versatile synthetic route to tailor the gelation behavior, pore structure, and the morphology of the final polymer network expanding the applicability of low density polymeric aerogels.

2. Experimental

2.1 Materials and general characterization

Dicyclopentadiene (DCPD, Aldrich), norbornene (NB, 99%, Aldrich), 5-norbornene-2-methanol, (**3**, 98%, Aldrich), 5-norbornene-2-*exo*,3-*exo*-dimethanol (**10**, 97%, Aldrich) and a first generation Grubbs' catalyst, bis(tricyclohexylphosphine)benzylidene ruthenium dichloride (+97%, Aldrich), and other chemicals were used as received unless noted otherwise. As supplied, the DCPD and monomer **3** are a mixture of mostly *endo* and *exo* isomers. They were used without further purification. Toluene (anhydrous, 99.8%, Aldrich) was degassed by bubbling with high purity nitrogen prior to use.

¹H NMR spectra were obtained with a Bruker Avance 600 instrument at 600 MHz. Rheological properties of precursor solutions during the gelation were characterized with a Rheometrics Fluids Spectrometer RFS 8400 in a dynamic-time-sweep mode with a Couette geometry (a 17 mm radius cup and a 16 mm radius bob). Measurements were carried out at room temperature with a strain amplitude of 5% of the 1 mm gap between the cup and the bob and a frequency of 1 radian per second. To minimize solvent evaporation, the cup was covered with a custom built lid. The morphology of monolithic aerogels was investigated with a Jeol JSM-7401F scanning electron microscope (SEM) at an acceleration voltage of 2-3 kV in a lower secondary electron image (LEI) mode with no sputter coating. The 4 MV ion accelerator (NEC, model 4UH) at Lawrence Livermore National Laboratory was used to perform Rutherford backscattering spectrometry (RBS) measurements with 1.5 MeV ⁴He⁺ ions incident normal to the sample surface and backscattered into a detector at 164° relative to the incident beam direction. During the ion-beam analysis, samples were neutralized by co-irradiation with a 500 eV electron beam. Analysis of RBS spectra was done with stopping powers and scattering cross sections from the RUMP code¹⁵ with an assumption of a specimen composition of C₁₀H₁₂I_x. BET surface areas, pore volumes and pore size distributions were measured by nitrogen absorption porosimetry with a Micromeritics Instrument ASAP 2000 after degassing at 70 °C for 12 h. Bulk densities were calculated from the weight and the physical dimensions of samples.

2.2 Synthesis of norbornene-based cyclic olefin monomers

Scheme 1 summarizes the synthesis of the norbornene-based cyclic olefin crosslinker and comonomers used in this study. First, the norbornene-based crosslinker, 1,4-di(*exo*-bicyclo[2.2.1]hept-5-en-2-yl)benzene (**2**), was prepared as previously reported (Scheme 1a).¹⁶ Purification was carried out by column chromatography (ethyl acetate/hexanes) followed by re-crystallization in ethyl acetate. Next, several norbornene monomers with a different length of the alkyl group were prepared similarly to the synthesis of 5-methoxymethylbicyclo[2.2.1]hept-2-ene (**4**) (Scheme 1b).^{17,18} Other alkyl substituted norbornene-based monomers **5-7** were synthesized by reacting 5-norbornene-2-methanol (**3**) with corresponding alkyl halides such as hexyl bromide, dodecyl bromide, and benzyl bromide in the presence of sodium hydride. Purification of monomers was carried out by extraction followed by silica gel flash column chromatography. Finally, iodo-norbornene monomer **9** was prepared and used as a monomer with a strong electronic interaction. The synthesis of the iodo-norbornene monomers was accomplished by initially tosylating the corresponding norbornene alcohol **3** in the presence of 4-(dimethylamino)pyridine (DMAP) followed by tosyl displacement using sodium iodide (Scheme 1c).¹⁹⁻
²¹ As a practical way to double the number of chemical functionalities in one monomer, 5-norbornene-2,3-dimethanol **10** was used to prepare bis-tosylated norbornene monomer **11** and bisiodo-norbornene monomer **12** as a typical example of functional monomers for monitoring of gel formation. Full details of the synthesis and characterization of norbornene-based monomers are described in the Supporting Information.

2.3 Preparation of poly(dicyclopentadiene-*random*-substituted norbornene) p(DCPD-*r*-NB-R) aerogels

Low-density (0.02-0.05 g/cc) P(DCPD-*r*-NB-R) gels were prepared from a ring opening metathesis polymerization (ROMP) of DCPD and NB-R in toluene employing a first generation Grubbs' catalyst as

a catalyst/initiator (Scheme 2). Different P(DCPD-*r*-NB-R) (100/*x*) (wt/wt) copolymer wet-gels were obtained by controlling the feed ratios of DCPD and NB-R by weight. For example, to fabricate 50 mg/cc P(DCPD-*r*-NB-R) (100/20) (wt/wt) aerogels, separate 50 mg/cc solutions of DCPD and NB-R monomers in toluene were prepared and then mixed as needed (0.83 mL of the DCPD and 0.17 mL of the NB-R solution for a 100/20 wt/wt aerogel). After adding an aliquot of the catalyst (0.1 mg) dissolved in toluene, the mixture was gelled in a sealed vial under ambient conditions.

2.4 Supercritical CO₂ drying

Wet gels were first placed into an agitated acetone bath for 2-3 days and then transferred to a Polaron critical point dryer. Acetone-filled gels were exchanged with a continuous flow of liquid CO₂ at 850 psi. Once the solvent was completely removed, the temperature and pressure in the dryer were increased to the supercritical regime (50 °C and ~1500 psi) and kept for 2-4 hr. The pressure was then allowed to slowly decrease to atmospheric pressure while keeping the temperature constant. Dry aerogels were subsequently recovered by slowly cooling down to room temperature.

3. Results and discussion

Considering that pure PDCPD polymers have a partially cross-linked structure,²²⁻²⁹ our approach was to control the degree of crosslinking in the polymer backbone through either (i) the use of a more reactive crosslinker to increase the crosslinking density or (ii) the copolymerization of DCPD with a linear monomer to decrease the degree of crosslinking. The norbornene-based crosslinker **2** was first used as a control to overcome the inherent limitation in crosslinking of DCPD molecules. Scheme 1a shows the synthesis of norbornene-based crosslinker **2** from a carbon-carbon coupling reaction of norbonadiene **1** with diiodobenzene, as previously reported.¹⁶ Second, various cyclic-olefin monomers,

NB-R, were prepared from 5-norbornene-2-methanol (**3**) and 5-norbornene-2,3-dimethanol (**10**) in order to investigate the effect of a pendant group on the morphology of gels (scheme 1b and 1c). The alcohol functionalized norbornene monomers can be used to form derivatives having various functional groups, as previously reported.^{17,18} Norbornene-based monomers were selected for their mild polymerization conditions and ability to form statistical copolymers with dicyclopentadiene rings. In this study, we prepared alkyl norbornene monomers (**4-7**) by protecting a pendant alcohol group with various alkyl halides including methyl iodide, hexyl bromide, dodecyl bromide, and benzyl bromide, respectively (Scheme 1b). Based on the difference in the polarity of reactant **3** and the protected adducts **4-7**, thin layer chromatography (TLC) and column chromatography were used for the analysis and purification of the crude product. ¹H NMR spectra before and after the protection reaction show the characteristic shift of peaks assigned to -C(2)H-, -C(2)H-CH₂O-R, and -C(5)H=C(6)H- bonds. Finally, a norbornene monomer **8** with a good leaving group was prepared from the reaction of **3** with *p*-toluenesulfonyl chloride (TsCl) in the presence of a base such as triethylamine (TEA), pyridine, or 4-(dimethylamino)pyridine (DMAP) (Scheme 1c). The use of DMAP or pyridine was found to be suitable to promote the reaction and led to a quantitative tosylation, while TEA resulted only in a partial conversion. This reaction was monitored by ¹H NMR spectroscopy, in which the resonance at 5.90 ppm, 3.75-3.30 ppm and 2.30-1.60 ppm, corresponding to -C(5)H=C(6)H-, -C(2)H-CH₂OH, and -C(2)H- in **3**, respectively, clearly shifted to 5.69 ppm, 4.08-3.57 ppm, and 2.40-1.73 ppm without overlapping those of the starting material. Norbornene activated with a good leaving group provides us with a useful platform for the introduction of additional chemical functionalities in the polymer. For example, iodonorbornene monomer **9** was prepared by reacting monomer **8** with sodium iodide. This reaction was confirmed from the change in the chemical shift and the disappearance of -OTs at 7.78-7.34 ppm. Norbornene-diol monomer **10** was also selected as a starting material to double the number of functionalities in one monomer. Direct reaction of monomer **10** with TsCl and subsequent precipitation

of the mixture in diethyl ether gave bis-tosylated norbornene **11** as white powder. Further purification of the residual solution by column chromatography isolated mono-substituted tosyl norbornene and cyclic ether norbornene byproducts, as identified by ^1H NMR. Then monomer **11** was reacted with excess NaI and transformed into bisiodo-norbornene monomer **12** in quantitative yield.

Scheme 2 shows the synthetic scheme of P(DCPD-*r*-NB-R) copolymer gels from the ROMP reaction of a mixture of DCPD and NB-R in toluene. In proposing the chemical structure of copolymers, it is assumed that the strained norbornene-derived double bond in the DCPD monomer is much more reactive than the cyclopentene-derived double bond, and the olefin addition contributes to the formation of crosslinked PDCPD.²⁷ Modified PDCPD-based aerogels were prepared by controlling the composition of the mixture of cyclic-olefin monomers including DCPD and NB-R. The gelation behavior of the DCPD/NB-R mixture showed a dependency on the ratio of NB-R to DCPD as well as the concentration of olefin monomers and the catalyst, consistent with a previous study of pure PDCPD aerogels.^{10,13} Bulk PDCPD and P(DCPD-*r*-NB-R) copolymer wet-gels were stable even after a few weeks, and pure NB solutions at the same condition did not form a gel. In the present study, the ratio of the catalyst to monomers and the total monomer concentration were fixed as 0.002 (wt/wt) and 50 mg/cc, respectively, unless otherwise noted. Both pure DCPD and mixtures of DCPD and NB-R were gelled at room temperature, and the catalyst did not appear to have any acute air or moisture sensitivity. It is worthy to mention that the use of a first generation Grubbs' catalyst over a second generation Grubbs' catalyst is due to its shorter gelation time in our typical experimental condition (not in a glove box). Typically, the addition of NB-R monomers increases the gelation time from ~10 min for pure DCPD to a few hours up to a few days. The addition of the NB-based crosslinker **2**, on the other hand, reduces the gelation time to ~1 min (see Table S1 in the Supporting Information). During the gelation of pure DCPD or **2**, there was a phase transition from transparent solution to an opaque gel due to the light scattering by polymerized wet gels. However, wet-gels prepared from a higher loading of the NB-R

monomer remained transparent after the gelation. All wet-gels were supercritically dried to form white monolithic aerogels.

The ability to form low-density thin film aerogel coatings with a thickness of $\sim 10\ \mu\text{m}$ to $100\ \mu\text{m}$ is crucial to our intended application. Recently, we reported on the effect of NB addition on the uniformity of PDCPD films.¹⁰ Here, we extend our study to higher NB concentrations and to other NB-based monomers NB-R. For comparative purposes, we include our previous results in the following discussion. The effect of NB-R additions was first evaluated by studying the formation of thin films in rotating horizontal glass vials ($\sim 20\ \text{mL}$) containing a precursor solution (1 mL) on a compact roller system, commonly used in cell culture studies (Fig. 1). Fig. 1b through 1d show results of gel coating experiments with pure PDCPD in conjunction with a norbornene based crosslinker and P(DCPD-*r*-NB-R) copolymer gels. These figures reveal that pure PDCPD gels do not form monolithic thin films under this condition, instead, the vial is coated with irregularly-shaped small lumps of the gel and contained a significant amount of fluid suggesting that the lumps consist of a higher density gel. The norbornene based crosslinker **2** does not show the superfluous fluid, but does not form a film probably due to its extremely fast gelation behavior. In sharp contrast, a uniform coating of a transparent wet-gel layer on the inside wall of a glass vial was observed from P(DCPD-*r*-NB-R) (100/20) at 50 mg/cc, regardless of the structure of -R substituents. In order to understand this unique change in gelation behavior under rotation and shear, we investigate the effect of the norbornene addition on rheological properties of P(DCPD-*r*-NB) gels, as shown in Fig. 1e through 1g (Fig. S1 in the Supporting Information). Isothermal dynamic time tests at a given frequency and strain show that both shear moduli and complex viscosity increase over time. A sudden increase in moduli and viscosity in a short period time is a typical change in gelation. In this study, we determined the gel point, or the initial formation of an infinite network, to be the time when the storage shear modulus, G' , exceeds the loss shear modulus, G'' ,²⁴ although several different protocols have been reported in literatures.³⁰ Our rheological

measurements reveal that the time at which G' and G'' cross over drastically increases with increasing NB concentration up to 10 wt % and then levels off even after further NB addition. Both moduli and viscosity at the crossover point increase almost linearly up to 40 wt %, as summarized in Table 1. The higher viscosity of P(DCPD-*r*-NB) near the gelation point reduces the shear experienced by the growing polymer network and makes it possible to fabricate a uniformly coated wet-gel layer on specific substrates, as reported in our previous work.¹⁰ BET surface areas and bulk densities of aerogel samples are also summarized in Table 1. It is worthy to mention that norbornene has a much higher ROMP reactivity (k_{obs} of 0.42 s⁻¹) than *endo*-DCPD (k_{obs} of 0.019 s⁻¹) at the same condition.²² Surprisingly, the gel time for PDCPD (491 s) is shorter than for P(DCPD-NB) gels (~2100 s). Although PDCPD aerogels show no volume change during gelation and supercritical CO₂ drying process, we observe that the measured density (~37 mg/cm³) is lower than the target density (~50 mg/cm³). This suggests incomplete conversion of monomers to gels, for example due to the early precipitation of highly crosslinked PDCPD networks caused by their limited solubility in toluene. Some amounts of shrinkage of gels during the acetone exchange process and the CO₂ drying process were observed in P(DCPD-*r*-NB) samples with more than 20 wt% NB, causing a sudden decrease in BET surface areas and a deviation from the target bulk density (see Fig. S2 in the Supporting Information). Preventing volume shrinkage at higher NB concentrations is the subject of current work that will be described in a future publication.

In addition to modifying the rheological behavior, the copolymerization also impacted the morphologies of PDCPD-based aerogels. Fig. 2a through 2c are SEM images of dried PDCPD aerogels with different DCPD concentrations of 50, 30, and 20 mg/cc. At a concentration lower than 10 mg/cc, the reaction was too slow to form gels within 7 days. Regardless of the target concentrations, pure PDCPD aerogels have a similar three-dimensional porous network of randomly oriented fibrous-shape structures with a non-uniform irregular pore structure.¹³ Copolymerization with norbornene (NB)

decreases the crosslinking density of pure PDCPD-based gels. Fig. 2d through 2f show the effect of the NB concentration (10 to 40 wt.%) on the morphologies of dried 50 mg/cc P(DCPD-*r*-NB). P(DCPD-*r*-NB) copolymer aerogels have a fibrous three-dimensional porous network similar to that of pure PDCPD. However, the length of individual fiber strands decreases from a few μm in the case of pure PDCPD to hundreds of nm in P(DCPD-*r*-NB) gels with higher concentrations of the NB monomer. This is consistent with the observation that NB addition results in the formation of clear wet gels.

The effect of the monomer addition on the morphologies of aerogels was further explored by using various norbornene monomers (**NB-R**) containing substituted groups with different steric and electronic structures. Fig. 3a through 3c are typical SEM images of aerogels prepared from mixtures of DCPD and NB-R with a different length of alkyl groups derived from methyl iodide, hexyl bromide, and dodecyl bromide. P(DCPD-*r*-NB-R) aerogels prepared using monomer **4** (R = methyl) show the characteristic fibrous network morphology observed in pure PDCPD and P(DCPD-*r*-NB) at low NB concentrations, while monomers **5** and **6**, which contain a longer chain alkyl group, created aerogels with a shorter and more entangled network. Pure PDCPD formed a number of clusters of long linear ligaments, whose entanglement led to the development of large, irregular shaped pores. However, the addition of co-monomers such as NB and monomers **4-6** appears to have either reduced the length of ligaments or caused more entanglement between them, the result of which is drastically different pore shape and size. As shown in Fig. 3d to 3f, more drastic changes in not only the pore size but also pore morphology of aerogels were observed from the addition of co-monomers **7-9** that contain a strong hydrophobic or electronic interaction. The monomers **7** and **8** with benzyl and tosyl groups resulted in spherical pores with sizes of ~ 50 nm, while the addition of iodo-monomer **9** produced extended long fibers reminiscent of pure PDCPD (see Fig. S3 in the Supporting Information). It is worthy to mention that the norbornene-based crosslinker **2** with a similar reactivity of two norbornene rings does not accompany the unique fiber-like morphologies of PDCPD-based aerogels. It formed fine particulate morphology,

often observed in silica aerogels (see Fig. S4 in the Supporting Information).¹³ The effect of NB-R (or NB) monomer addition on the morphologies is schematically represented in Fig. 3g. The distinct features in P(DCPD-*r*-NB-R) copolymer networks are changes in length of fiber strands, and pore sizes and morphologies surrounded by the strands. Leventis et al.³¹⁻³³ explained the formation of organic (polymer) aerogels by (i) crosslinking at the molecular level resulting in early phase separation of small surface-reactive particles and (ii) subsequent inter-particle crosslinking that improves mechanical properties of the materials. Based on those principles, long PDCPD strands with a length of hundreds of nm up to a few μm would be the combination of primary and secondary particles like in polyurea aerogels.³² In this study, the incorporation of NB-R with a different substituent group might distort further growth of the primary PDCPD fibrils by either (i) decreasing the number of reactive sites (*i.e.*, the crosslinking) at the surface or (ii) sterically hindering inter-particle crosslinking, as has been proposed for polyimide aerogels from anhydride and isocyanates.³³ Formation of many shorter fiber strands with a good solubility and/or a better chain mobility makes it possible to form more entangled morphologies, and it could explain a transformation in the pore size and morphologies as well as the higher moduli and viscosity at the gel point of in the copolymer gel systems. Considering the effect of different crosslinkers, the unique fibril structure of primary particles seems to be attributed to the molecular structure of PDCPD and its inter-molecular interaction. In this regard, the effect of different DCPD stereo-isomers on morphologies is currently being investigated and will be a subject of further release. This result indicates that additional tuning over pore morphologies of polymeric aerogels could be gained by the copolymerization approach in conjunction with a careful design of co-monomers and/or cross-linkers. Full details on the morphologies of P(DCPD-*r*-NB-R) aerogels with a different composition are included in the Supporting Information.

The versatility of the copolymer networks derived from ring opening metathesis polymerization (ROMP) allows one to introduce chemical functionality by taking advantage of the tunability of the

NB-R co-monomer. For our specific application, a millimeter-sized spherical shell with a thin aerogel layer on the inside of the shell, the availability of a non-destructive imaging technique such as x-ray radiography is essential to judge the success of the coating experiment. This, however, requires increasing the weak x-ray absorption contrast of the CH-based foam by introducing a high-Z element. This motivated our effort to synthesize of the bisiodo-norbornene monomer **12** (Fig. 4a). Fig. 4b shows a photo of P(DCPD-*r*-**12**) aerogels with different wt. percentages, *a*, of monomer **12**. Monolithic aerogels were formed from the supercritical CO₂ drying process of P(DCPD-*r*-**12**). They did not show any serious shrinkage during the polymerization and drying process and retain the original shapes of PDCPD although a slight shrinkage occurred for high concentrations of monomer **12**. A typical SEM image of dried aerogels indicates that they have a fibrous-shape morphology, similar to other P(DCPD-*r*-NB-R) aerogels (Fig. 4c). The incorporation of iodine was verified with energy-dispersive X-ray spectroscopy (EDS) and the result is shown in Fig. 4d. Characteristic carbon and iodine EDS mapping images in Fig. 4e and 4f reveal a uniform distribution of iodine through the aerogels.

Further quantitative information on the material composition was obtained from Rutherford backscattering spectrometry (RBS) because of the unique ability of RBS to deliver highly accurate film composition without the use of standards. Fig. 5a shows a typical RBS spectrum of P(DCPD-*r*-**12**) (100/100) acquired with an analyzing ion dose of $\sim 8 \times 10^{12} \text{ cm}^{-2}$. We found that the iodine concentration in aerogels increased with the concentration of monomer **12** in the copolymer, as anticipated. However, we also found that He⁺ ion irradiation during the RBS analysis resulted in composition changes, as shown in Fig. 5b. Thus, the initial sample composition at zero dose of the analyzing beam for each sample was determined by extrapolating dose dependencies. The iodine concentrations in P(DCPD-*r*-**12**) (100/20) and (100/100) samples were determined to be about 0.63 and 1.90 (at.%), respectively. From the assumption of the chemical structure of P(DCPD-*r*-**12**) (Fig. 5c), the RBS result is used to determine the molar ratios of NB-R to DCPD in copolymer gels (see the details in the Supporting Information).

These values correspond to (100/21) and (100/75) by weight, respectively. This shows that comonomers were uniformly incorporated throughout polymer gels within a relatively good yield from feed ratios.

4. Conclusion

In summary, we have explored the potential of ring opening metathesis polymerization (ROMP) as a simple and efficient synthetic route to polymeric aerogels with a target density of 0.02-0.05 g/cm³. The copolymerization of dicyclopentadiene (DCPD) with various substituted norbornene (NB-R) monomers highlights the versatility of the ROMP approach. Significant enhancements in coating behavior observed for P(DCPD-*r*-NB-R) copolymer gels make it possible to fabricate uniform low density polymeric aerogel coatings on various substrates. The copolymerization approach can also be used to modify the pore structure and morphology of aerogels as well as to introduce chemical functionality. The approach described herein could potentially expand the use of hydrocarbon aerogel materials in a wide range of applications in the fields of material, environmental, and industrial science.

Acknowledgments

This work performed under the auspices of the U.S. Department of Energy by Lawrence Livermore National Laboratory under Contract DE-AC52-07NA27344. We thank Dr. Brian P. Mayer and Dr. Ian D. Hutcheon for their valuable assistance in the execution of NMR and SEM experiments.

Electronic supplementary information (ESI) available: Details on the experimental procedure for the synthesis of cyclic olefin monomers, rheological measurements of G' , G'' , and η^* during the gelation of P(DCPD-*r*-NB) (100/*x*) samples, procedure to determine molar ratios of NB-R to DCPD in

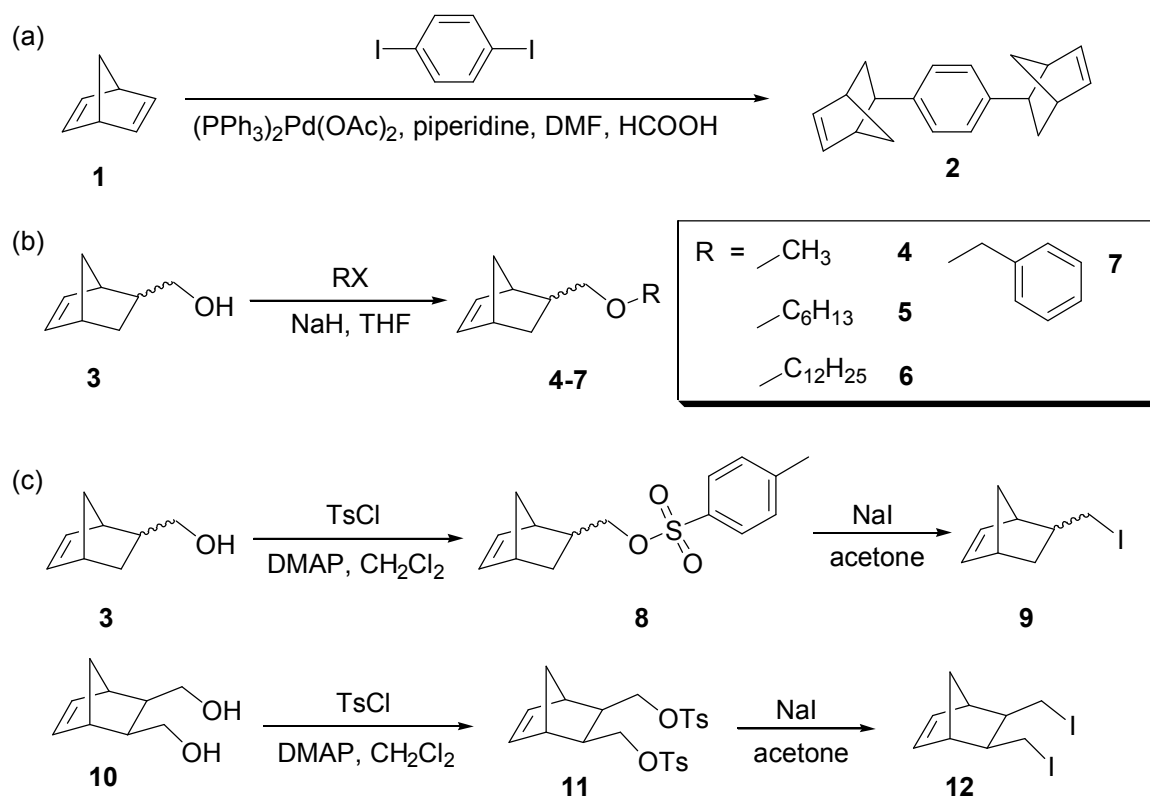
copolymer gels from RBS results, and the gel time, photos, and morphologies of P(DCPD-*r*-NB-R) with a different composition.

Table 1 General characteristics of P(DCPD-*r*-NB) aerogels

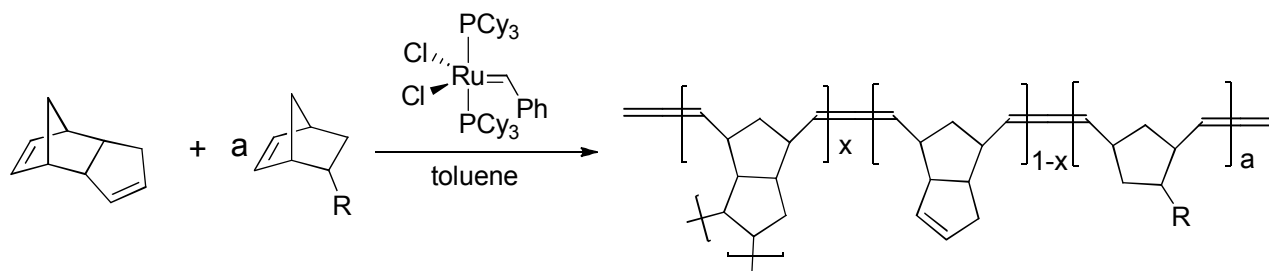
Sample	Feed ratio of DCPD to NB ^a		t_{gel}^b (s)	G'_{gel}^b (Pa)	$\eta^*_{\text{gel}}^b$ (Pa·s)	Surface area ^c (m ² /g)	Total pore volume ^c (m ² /g)	Bulk density ^d (mg/cm ³)
	by weights	by moles						
P(DCPD- <i>r</i> -NB)	100:0	100:0	491	0.07	0.08	103	0.31	37±4
	100:10	100:14	2086	7.45	10.53	114	0.21	48±8
	100:20	100:28	2110	11.22	15.81	102	0.19	82±13
	100:30	100:42	2148	16.45	23.23	57	0.07	102±37
	100:40	100:56	2055	20.97	29.59	22	0.02	244±48

^a DCPD and NB monomers were separately dissolved to have a concentration of 50 mg/cc in toluene and mixed to be a final composition. ^b The gel point of the system was determined from the crossover of the storage shear modulus, G' , and the loss shear modulus, G'' , measured by rheometry. ^c Surface area and total pore volume of aerogels measured by BET. ^d Bulk densities were calculated from the weight and the physical dimensions and averaged with the multiple sample measurement

Scheme 1 Synthesis of Cyclic Olefin Monomers



Scheme 2 Ring Opening Metathesis Polymerization of DCPD and NB-R



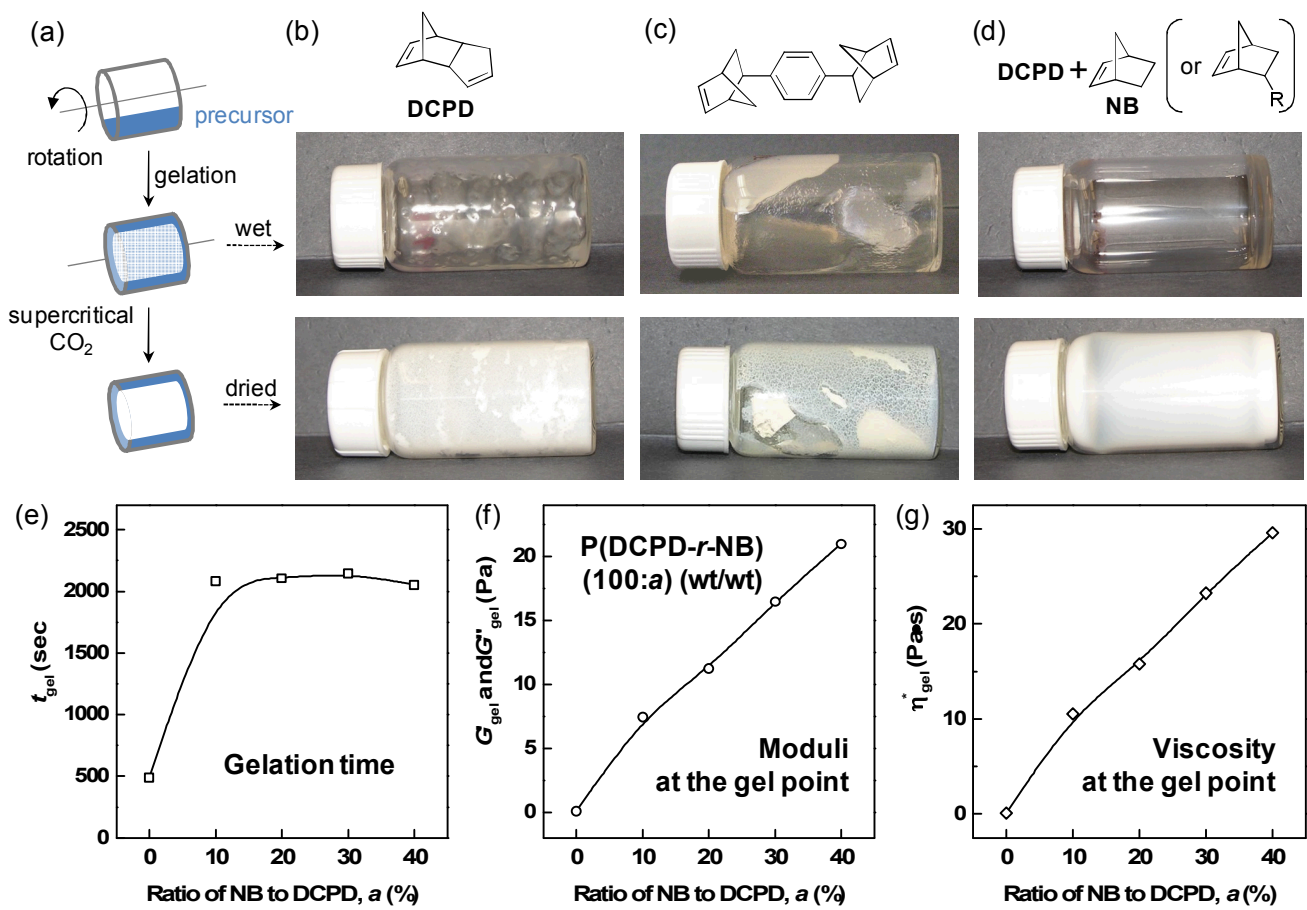


Fig. 1 (a) Schematic representation of the coating experiment of precursor solution. (b-d) Typical examples of the formation of wet-gel and supercritical CO₂ dried aerogel films prepared from pure DCPD, a multi-norbornene (*n*NB)-based crosslinker, and a mixture of DCPD and NB (or NB-R). (e-g) Influence of NB addition on the formation of P(DCPD-*r*-NB) copolymer gels under shear and the rheological properties of shear moduli and complex viscosity at the gel point.

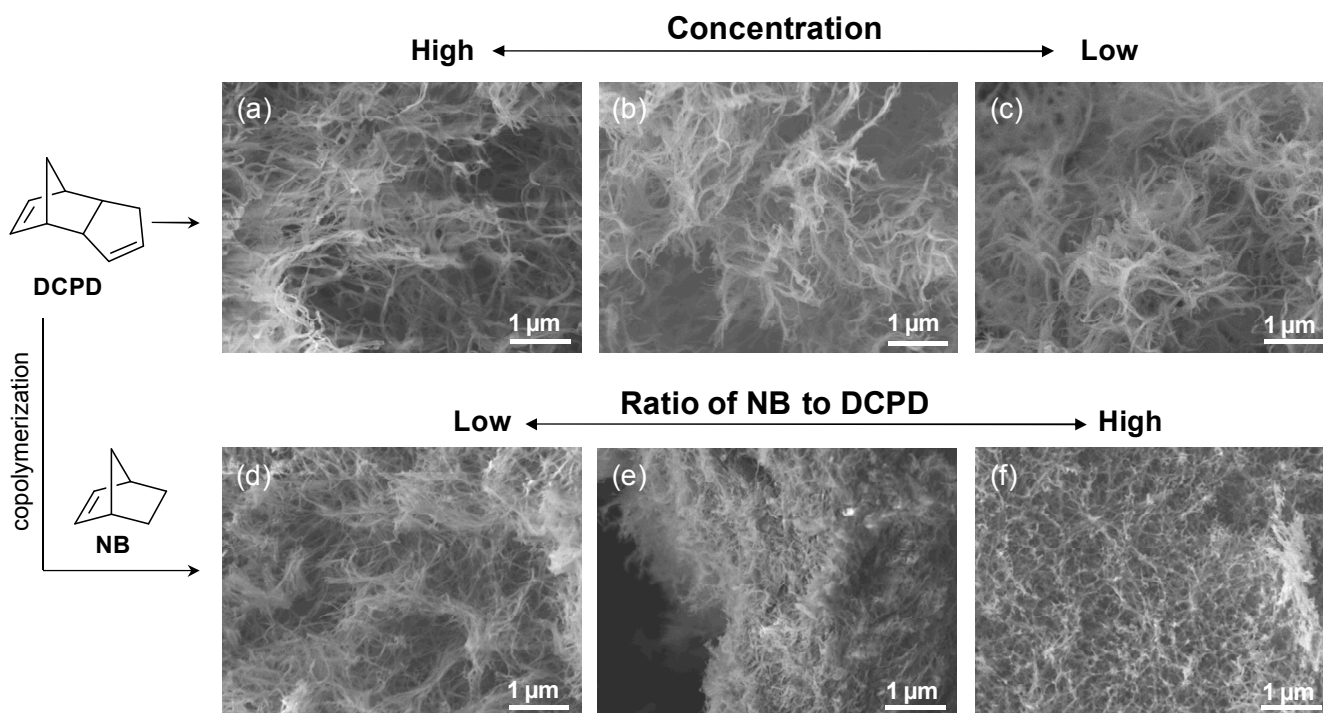


Fig. 2 Effect of the composition of precursor solutions on aerogel morphologies. (a-c) Pure PDCPD aerogels prepared from (a) 50, (b) 30, and (c) 20 mg/cc solutions and (d-f) P(DCPD-*r*-NB) copolymer aerogels prepared from mixtures with different DCPD/NB ratios of (d) (100/10), (e) (100/20), and (f) (100/40) (wt/wt) at 50 mg/cc.

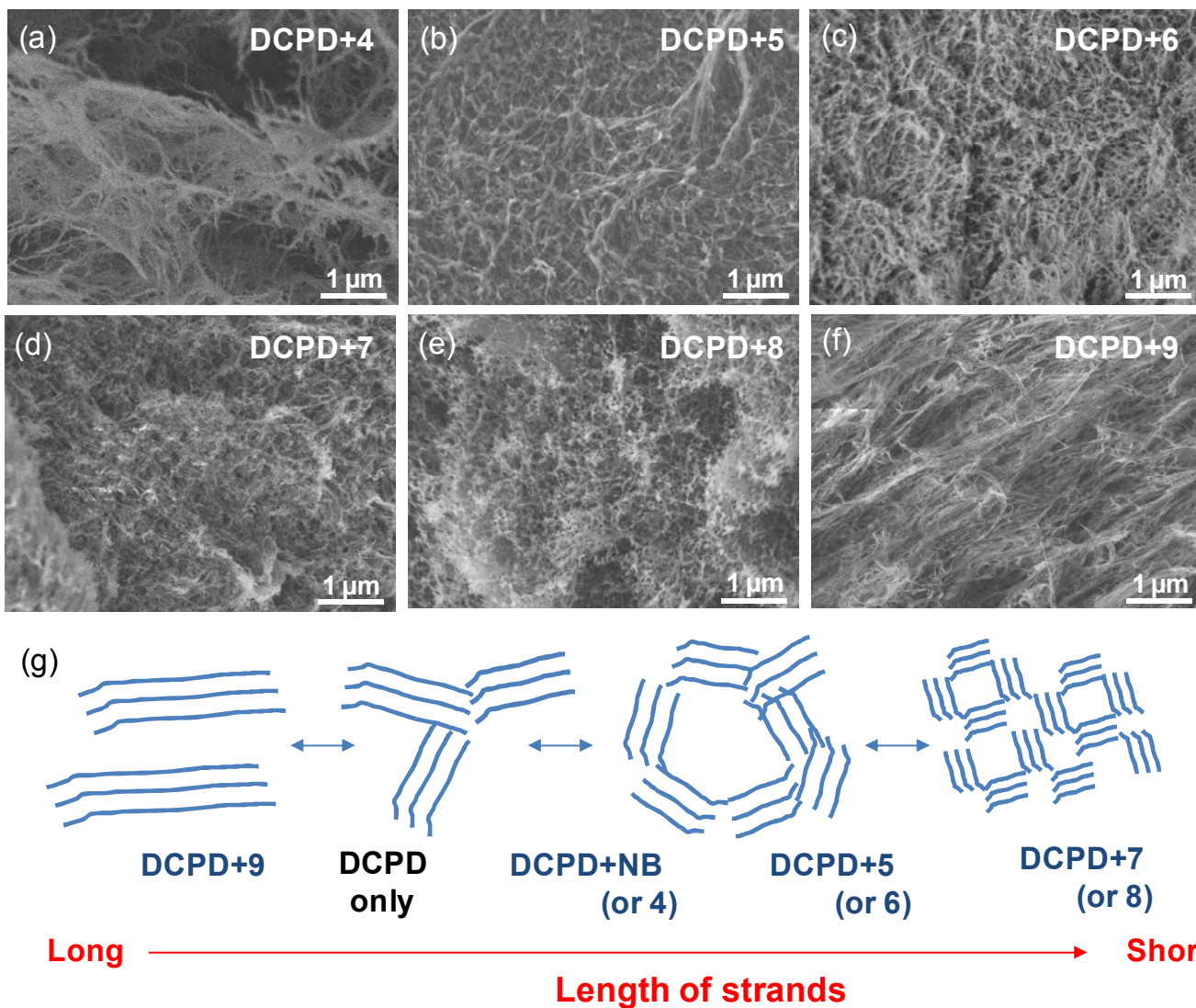


Fig. 3 (a-f) Characteristic morphologies of P(DCPD-*r*-NB-R) aerogels prepared from mixture of DCPD with a different NB-R co-monomer: (a) DCPD+4, (b) DCPD+5, (c) DCPD+6, (e) DCPD+7, (f) DCPD+8, and (g) DCPD+9. (g) Proposed model for representing the effect of NB-R monomer on the formation of P(DCPD-*r*-NB-R) aerogels with different morphologies.

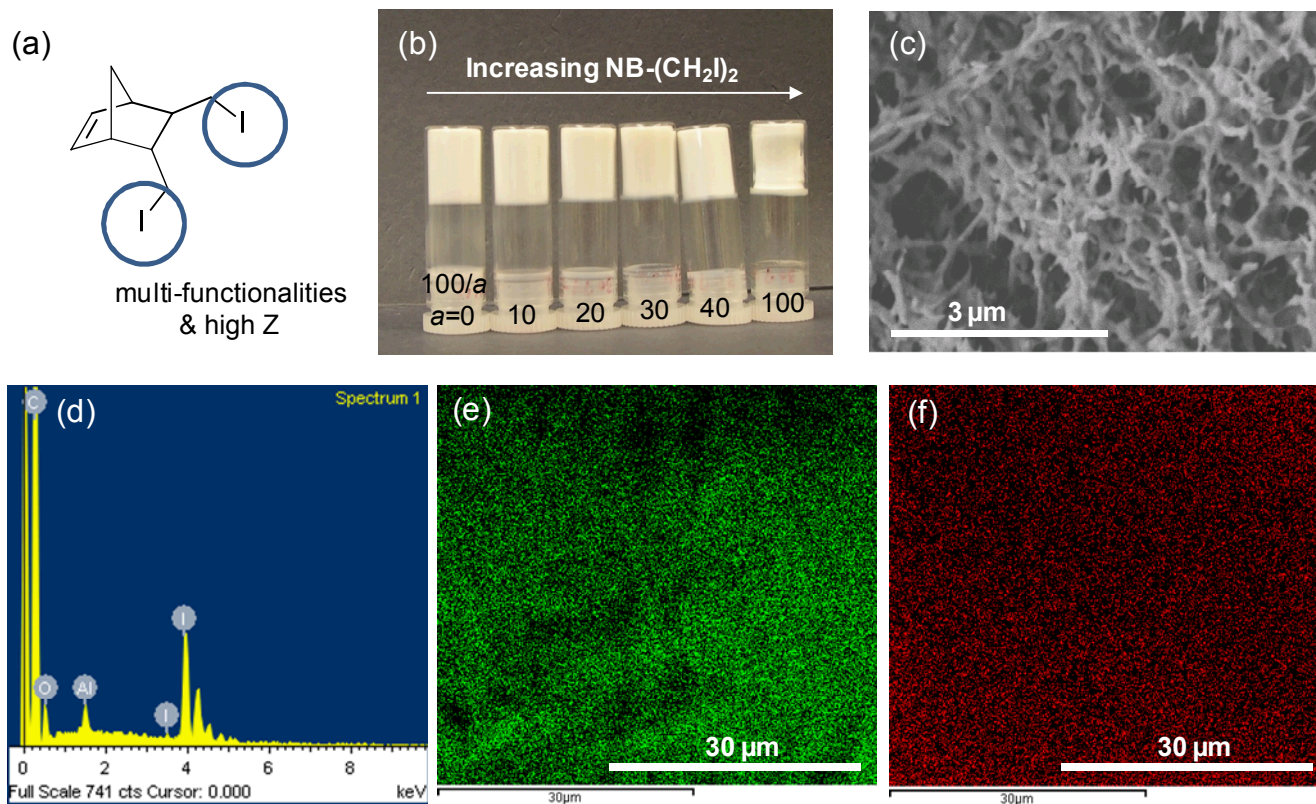


Fig. 4 Introduction of chemical functionality into aerogels: (a) bisiodo norbornene monomer **12** as an example of a functional monomer, (b) a photo of dried P(DCPD-*r*-**12**) (100/*a*) (wt/wt) monoliths, (c-f) typical examples of (c) SEM image and (d) energy-dispersive X-ray spectrum (EDS), (e) C-mapping and (f) I-mapping images on P(DCPD-*r*-**12**) (100/100) aerogel.

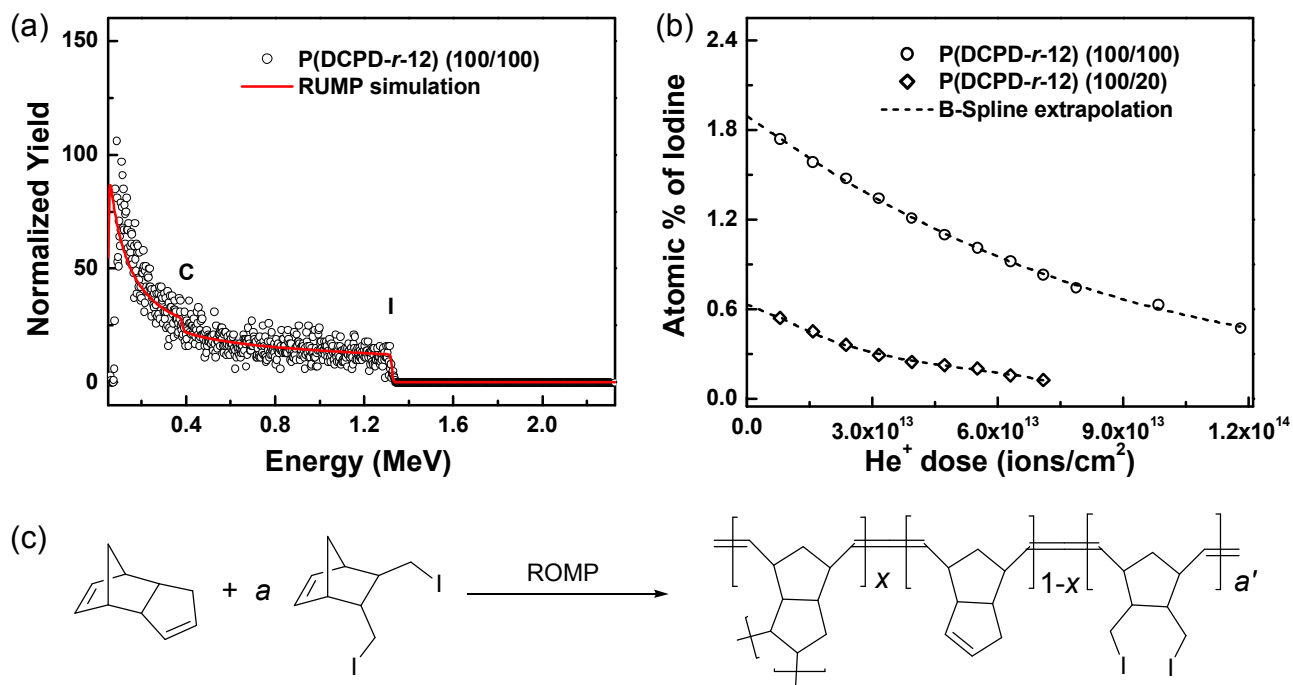


Fig. 5 Rutherford backscattering spectrometry (RBS) analysis of P(DCPD-*r*-12) (100/*a*) (wt/wt) aerogels: (a) A typical RBS spectrum (symbols) and a RUMP-code simulation (solid line), (b) the atomic concentration of iodine in P(DCPD-*r*-12) samples as a function of the dose of the analyzing ion beam (1.5 MeV He), and (c) Chemical structure of P(DCPD-*r*-12) used for the determination of the composition of samples.

References

- 1 R. W. Pekala, *J. Mater. Sci.*, 1989, **143**, 3221-3227.
- 2 W. W. Lukens and G. D. Stucky, *Chem. Mater.*, 1989, **14**, 1665-1670.
- 3 S. Bag, I. U. Arachchige and M. G. Kanatzidis, *J. Mater. Chem.* 2008, **18**, 3628-3632.
- 4 D. R. Rolison, J. W. Long, J. C. Lytle, A. E. Fischer, C. P. Rhodes, T. M. McEvoy, M. E. Bourg and A. M. Lubers, *Chem. Soc. Rev.*, 2009, **38**, 226-252.
- 5 J. Biener, M. Stadermann, M. Suss, M. A. Worsley, M. M. Biener, K. A. Ross and T. F. Baumann, *Energy Environ. Sci.*, 2011, **4**, 656-667.
- 6 K. Nagai, H. Azechi, F. Ito, A. Iwamoto, Y. Izawa, T. Johzaki, R. Kodama, K. Mima, T. Mito, M. Nakai, N. Nemoto, T. Norimatsu, Y. Ono, K. Shigemori, H. Shiraga and K. A. Tanaka, *Nucl. Fusion*, 2005, **45**, 1277-1283.
- 7 K. Nagai, T. Norimatsu and Y. Izawa, *Fusion Sci. Technol.*, 2004, **45**, 79-83.
- 8 U. Meyer, F. Svec, J. M. J. Fréchet, C. J. Hawker and K. Irgum, *Macromolecules*, 2000, **33**, 7769-7775.
- 9 J. Streit and Schroen, D., *Fusion Sci. Technol.*, 2003, **43**, 321-326.
- 10 C. Dawedeit, S. H. Kim, T. Braun, M. A. Worsley, S. A. Letts, K. J. Wu, C. C. Walton, A. A. Chernov, J. H. Satcher Jr., A. V. Hamza and J. Biener, *Soft Matter*, 2012, **8**, 3518-3521;

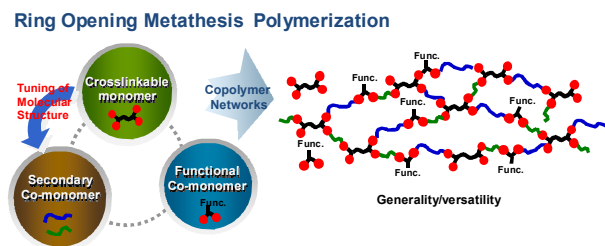
- 11 J. Biener, C. Dawedeit, S. H. Kim, T. Braun, M. A. Worsley, A. A. Chernov, C. C. Walton, T. M. Willey, S. O. Kucheyev, S. J. Shin, Y. M. Wang, M. M. Biener, J. R. I. Lee, B. J. Koziolowski, T. van Buuren, K. J. J. Wu, J. H. Satcher Jr. and A. V. Hamza, *Nucl. Fusion*, 2012, **52**, 062001.
- 12 (a) P. A. Levkin, F. Svec and J. M. J. Frechet, *Adv. Funct. Mater.*, 2009, **19**, 1-6; (b) J. Hiller, J. D. Mendelsohn and M. F. Rubner, *Nat. Mater.*, 2002, **1**, 59-63.
- 13 J. K. Lee and G. L. Gould, *J. Sol-Gel Sci. Technol.*, 2007, **44**, 29-40.
- 14 (a) N. Leventis, C. Sotiriou-Leventis, D. P. Mohite, Z. J. Larimore, J. T. Mang, G. Churu and H. Lu, *Chem. Mater.*, 2011, **23**, 2250-2261; (b) D. P. Mohite, Z. Larimore, C. Sotiriou-Leventis and N. Leventis, 242nd National Meeting of the American-Chemical-Society (185-PMSE), Denver, 2011.
- 15 L. R. Doolittle, *Nucl. Instrum. Meth. B*, 1985, **9**, 344-351.
- 16 A. G. M. Barrett, B. T. Hopkins, A. C. Love and L. Tedeschi, *Org. Lett.*, 2004, **6**, 835-837.
- 17 S. D. Drouin, F. Zamanian and D. E. Fogg, *Organometallics*, 2001, **20**, 5495-5497.
- 18 A. Bell, B. Knapp, D. Jablonski and P. W. Newsome, *US Pat.*, 0 099 906, 2010.
- 19 D. D. Reynolds and W. O. Kenyon *J. Am. Chem. Soc.*, 1950, **72**, 1593-1596.
- 20 T. W. Gibson and W. F. Erman, *J. Am. Chem. Soc.*, 1969, **91**, 4771-4778.
- 21 J. J. Gajewski and J. L. Jimenez, *J. Am. Chem. Soc.*, 1986, **108**, 468-474.
- 22 Vougioukalakis, G. C. and R. H. Grubbs, *Chem. Rev.*, 2010, **110**, 1746-1787.
- 23 S. R. White, N. R. Sottos, P. H. Geubelle, J. S. Moore, M. R. Kessler, S. R. Sriram, E. N. Brown and S. Viswanathan, *Nature*, 2001, **409**, 794-797.

- 24 X. Sheng, J. K. Lee and M. R. Kessler, *Polymer*, 2009, **50**, 1264-1269.
- 25 X. Sheng, M. R. Kessler and J. K. Lee, *J. Therm. Anal. Calori.*, 2007, **89**, 459-464.
- 26 A. D. Martina, J. G. Hilborn and A. Mühlebach, *Macromolecules*, 2000, **33**, 2916–2921.
- 27 T. A. Davidson, K. B. Wagener and D. B. Priddy, *Macromolecules*, 1996, **29**, 786–788.
- 28 J. D. Rule and J. S. Moore, *Macromolecules*, 2002, **35**, 7878–7882.
- 29 P. J. Hine, T. Leejarkpai, E. Khosravi, R. A. Duckett and W. J. Feast, *Polymer*, 2001, **42**, 9413-9422.
- 30 P. J. Halley and M. E. Mackay, *Pol. Eng. Sci.*, 1996, **36**, 593-609.
- 31 (30) N. Leventis, C. Chidambareswarapattar, D. P. Mohite, Z. J. Larimore, H. Lu and C. Sotiriou-Leventis, *J. Mater. Chem.* 2011, **21**, 11981-11986.
- 32 N. Leventis, C. Sotiriou-Leventis, N. Chandrasekaran, S. Mulik, Z. J. Larimore, H. Lu, G. Churu and J. T. Mang, *Chem. Mater.*, 2010, **22**, 6692-6710.
- 33 C. Chidambareswarapattar, Z. Larimore, C. Sotiriou-Leventis, J. T. Mang, N. Leventis, *J. Mater. Chem.* 2010, **20**, 9666-9678.

Table of Contents

Exploration of the Versatility of Ring Opening Metathesis Polymerization: an Approach for Gaining Access to Low Density Polymeric Aerogels

Sung Ho Kim, Marcus A. Worsley, Carlos A. Valdez, Swanee J. Shin, Christoph Dawedeit, Tom Braun, Sergei O. Kucheyev, Theodore F. Baumann, Stephan A. Letts, Kuang Jen J. Wu, Juergen Biener, Joe H. Satcher Jr., and Alex V. Hamza



Development of a simple, powerful synthetic technique for polymeric aerogels and uniform aerogel coatings on non-planar surfaces was reported.